Journal of Alloys and Compounds 509 (2011) 6773–6776

Contents lists available at ScienceDirect

Journal of Alloys and Compounds

journal homepage: www.elsevier.com/locate/jallcom

Solubility of YbTe in Sb_2Te_3 and thermodynamic properties of the solid solution

Ziya S. Aliev[a], Gulnara I. Ibadova[a], Jean-Claude Tedenac[b], Andrei V. Shevelkov[c,*], Mahammad B. Babanly[a,**]

[a] Baku State University, General and Inorganic Chemistry Department, Baku, Azerbaijan
[b] University of Montpellier II, PMOF, ICGM UMR 5253, Montpellier, France
[c] Lomonosov Moscow State University, Chemistry Department, Moscow, Russia

ARTICLE INFO

Article history:
Received 29 January 2011
Received in revised form 18 March 2011
Accepted 1 April 2011
Available online 8 April 2011

Keywords:
Phase diagram
Solid solution
Electromotive force
Thermodynamic properties

ABSTRACT

The solubility of YbTe in Sb_2Te_3 is investigated by a combination of DTA, XRD, SEM, and EMF methods. The fragment of the *T–x* phase diagram of the YbTe–Sb_2Te_3 system is constructed for 0–25 mol.% YbTe. It is shown that the solubility limit for YbTe in Sb_2Te_3 is achieved at 15 mol.% YbTe at 300 K and at 17.5 mol.% YbTe at 855 K. From the EMF measurements with an YbTe electrode the partial thermodynamic functions of the YbTe pseudo-component are calculated for the alloys of different compositions. Also, the standard integral thermodynamic functions of the YbTe dissolution in Sb_2Te_3 as well as the standard thermodynamic functions of formation and the standard entropy of the solid solution are calculated from the experimental data.

1. Introduction

Binary and ternary tellurides of heavy p-elements are low-gap semiconductors, which are deemed as "matrices" for creation of new and better thermoelectric materials [1–3]. These systems include tellurides of rare-earth metals and antimony or bismuth [4–6]. Recently, $YbSb_2Te_4$ was found to have perspective thermoelectric properties; the dimensionless figure-of-merit that characterizes its thermoelectric efficiency almost reaches 0.5 at 510 K [6]. The synthesis and investigation of the ytterbium antimony tellurides is hampered by the uncertainty of the ternary Yb–Sb–Te phase diagram. For instance, it was reported in the literature [4] that the YbTe–Sb_2Te_3 quasi-binary system contains two ternary compounds $YbSb_2Te_4$ and $YbSb_4Te_7$; the former melts with decomposition at 923 K, whereas the latter melts congruently at 943 K. It was proposed [4] that both compounds have structures related to the cubic Th_3P_4 type, which was not supported by any kind of structural investigation. On the contrary, the analysis of the X-ray powder diffraction pattern hinted for the layered hexagonal/trigonal structure of $YbSb_2Te_4$ [6], similar to the structure of $PbSb_2Te_4$, which is a 21-layer derivative of the tetradymite structure [7]. Moreover, although the solubility of YbTe in Sb_2Te_3 was reported not to exceed 6 mol.% [4], this value is doubtful as soon as the achievement of equilibrium was not controlled properly in that work, and the admixtures of YbTe can be clearly viewed on the reported XRD patterns.

The creation of new thermoelectric materials with optimized properties requires controlling over their chemical composition and knowledge of their chemical properties and synthetic pathways. Keeping this in mind, we present in this work the results of the experimental determination of solubility of YbTe in Sb_2Te_3 and thermodynamic parameters of the corresponding solid solution. This work is a step on the way to new telluride-based thermoelectric materials with optimized properties.

2. Experimental

The binary compounds Sb_2Te_3 and YbTe were synthesized by melting stoichiometric amounts of the pure elements Sb (99.999%), Yb (99.99%), and Te (99.999%) in sealed silica and niobium tubes, respectively, according to the literature procedures [4,8]. The quality of the synthesized compounds was checked using DTA and XRD analysis, which confirmed their purity. Alloys in the YbTe–Sb_2Te_3 system with 5, 10, 12.5, 15, 17.5, 20, 22.5, and 25 mol.% YbTe were prepared by melting the stoichiometric quantities of the pre-synthesized binary tellurides. The starting mixtures were sealed in niobium tubes under vacuum (~10^{-2} Pa) such that the free volume was minimized and heated to 1000 K. Then the resulting melts were cooled down to 820 K and annealed at 820 K for about 2000 h to achieve equilibrium. Throughout the annealing temperature was controlled and maintained within the accuracy of 2 K, ensuring that no volatile component leaves the sample and that the composition of the resulting alloys strictly corresponds to the stoichiometry of the starting mixture.

Differential thermal analysis (DTA) was performed using the NTR-70 pyrometer equipped with chromel–alumel thermocouples, with the ramp rate of 7–8 K min^{-1}. X-ray powder diffraction (XPD) analysis was done with the X'Pert MPD Difractometer (Cu-K_α radiation). Scanning electron microscope Philips-XL30FEG was employed for the microstructure analysis.

* Corresponding author at: Leninskie Gory 1-3, Moscow 119991, Russia.
** Corresponding author at: Z. Khalilov Str. 23, Baku, AZ 1148, Azerbaijan.
E-mail addresses: shev@inorg.chem.msu.ru (A.V. Shevelkov), babanly_mb@rambler.ru (M.B. Babanly).

0925-8388/$ – see front matter © 2011 Elsevier B.V. All rights reserved.
doi:10.1016/j.jallcom.2011.04.025

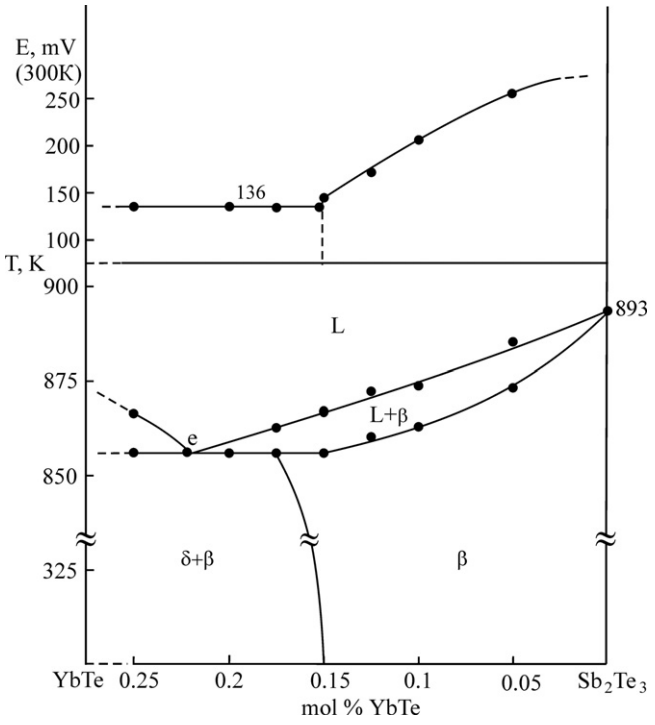

Fig. 1. A fragment of the phase diagram for the system YbTe–Sb_2Te_3 (bottom) and the concentration dependence of the EMF for the chains of type (1) (top).

Electromotive force (EMF) measurements were performed for the reversible concentration chains

$$(-)\ \text{YbTe}\ (s)|\text{liquid electrolyte},\ \ Yb^{+3}|(\text{Yb–Sb–Te})\ (s)\ (+) \qquad (1)$$

In the chains (1), YbTe with the 0.01 at.% excess of tellurium was used as the left electrode; the equilibrium alloys of the YbTe–Sb_2Te_3 systems with the desired composition were used as the right electrode. The electrodes were prepared by pressing the alloys onto molybdenum contacts in the form of cylinders with the mass of 0.5 g. The solution of chemically pure anhydrous $CaCl_2$ in glycerin was used as the electrolyte. Prior to use, analytically pure glycerin was degassed and dried by pumping at 400 K to remove traces of water and oxygen. EMF was measured by the compensation method in the temperature range of 300–400 K, using the high-resistance universal B7-34A digital voltmeter. In each experiment the first reading was performed after keeping the electrochemical cell at 380 K for 40–60 h, and then 3–4 h after reaching each desired temperature, which ensures the achievement of equilibrium. The construction of the electrochemical cell and the measuring procedure are described in detail elsewhere [9,10].

All our attempts to perform EMF study with the concentration chains based on metallic ytterbium failed. We observed sharp drop of the voltage from the starting values of about 1000 mV to 400–600 mV, although the expected value should have been higher than 800 mV [8].

3. Results and discussion

3.1. Solubility of YbTe in Sb_2Te_3

Based on the DTA data obtained using the annealed alloys, the fragment of the YbTe–Sb_2Te_3 phase diagram (0–25 mol.% YbTe) is constructed (Fig. 1). It is clear the solubility limit of YbTe in Sb_2Te_3 ranges from 15 mol.% at 300 K to 17.5 mol.% at 855 K; from here on this solid solution is named the β-phase. The eutectic point is found to have the composition corresponding to 22 mol.% YbTe. The two-phase region below the eutectic line seems to consist of the β-phase and the solid solution based on $YbSb_4Te_7$, which is labeled the δ-phase according to the literature [5].

Table 1
Temperature dependence of EMF for the chains of type (1) in the range of 300–400 K.

Phase composition	$E\,(\text{mV}) = a + bT \pm 2S_E(T)$
β (5 mol.% YbTe)	$223.1 + 0.118T \pm 2\left[\frac{2.4}{22} + 7.5\times10^{-5}(T-362.8)^2\right]^{1/2}$
β (10 mol.% YbTe)	$171.6 + 0.124T \pm 2\left[\frac{1.6}{22} + 5.1\times10^{-5}(T-362.8)^2\right]^{1/2}$
β (15 mol.% YbTe)	$100.7 + 0.136T \pm 2\left[\frac{1.7}{22} + 5.5\times10^{-5}(T-362.8)^2\right]^{1/2}$

The XRD data confirm that the alloys containing up to 15 mol.% YbTe are single-phase, whereas the alloys having from 17.5 to 25 mol.% YbTe contain admixtures (Fig. 2). The XRD patterns for different YbTe contents within the β-phase resemble that of pure Sb_2Te_3, the only difference being the peak positions. Upon increasing the YbTe content, the rhombohedral unit cell parameters decrease only slightly. For instance, the addition of 10 mol.% YbTe gives the following decreasing of the unit cell parameters compared to the pristine Sb_2Te_3: $\Delta a = 0.015$ Å and $\Delta c = 0.05$ Å. The analysis of the XRD patterns of the two-phase alloys (17.5–25 mol.% YbTe) confirms that the side phase does not show structural similarities with the cubic Th_3P_4 type. Rather, it has another variant of the layered structure typical for antimony and bismuth chalcogenides and chalcogen-halides [1,7,11]. Further confirmation of the XRD results comes from the SEM data. Fig. 3 clearly shows that the sample with 15 mol.% YbTe is phase-pure, whereas the alloy having 20 mol.% YbTe consists of two phases.

The results of the EMF measurements for the chains of type (1) allowed us more accurate determination of the concentration limit for the β-phase (Fig. 1). The voltage was found to decrease upon increasing the YbTe content up to 15 mol.%. At higher YbTe content, the voltage remains constant irrespective of the alloy composition. The constancy of the voltage in the two-phase region points at the unchangeable composition of two phases coexisting under equilibrium conditions.

3.2. Thermodynamic functions

The linear least-square treatment of the EMF data was performed [12] and the results were expressed according to the literature recommendations [13] as

$$E = a + bT \pm t\left[\frac{\delta_E^2}{n} + \delta_b^2(T-\bar{T})^2\right]^{1/2}, \qquad (2)$$

where n is the number of pairs of E and T values; δ_E^2 and δ_b^2 are the error variances of the EMF readings and b coefficient, respectively; $\bar{T}$ is the mean absolute temperature; t is the Student's test, which does not exceed 2 for $n \geq 20$ at the confidence level of 95% [12]. Table 1 summarizes the results for different YbTe contents within the β-phase. Using these equations the relative partial thermodynamic functions of the pseudo-component YbTe in the β-phase at 298 were calculated (Table 2). In fact, these functions are the difference between the partial molar functions of Yb in YbTe and

Table 2
Partial thermodynamic functions of the YbTe pseudo-component in the solid solution $(YbTe)_x(Sb_2Te_3)_{1-x}$ at 298 K.

Phase composition	$-\overline{\Delta G}_{YbTe}$ (kJ mol^{-1})	$-\overline{\Delta H}_{YbTe}$ (kJ mol^{-1})	$\overline{\Delta S}_{YbTe}$ (J K^{-1} mol^{-1})
β (5 mol.% YbTe)	74.762 ± 0.360	64.58 ± 1.82	34.16 ± 5.01
β (10 mol.% YbTe)	60.373 ± 0.297	49.67 ± 1.50	35.89 ± 4.13
β (15 mol.% YbTe)	40.886 ± 0.308	29.49 ± 1.56	39.37 ± 4.29

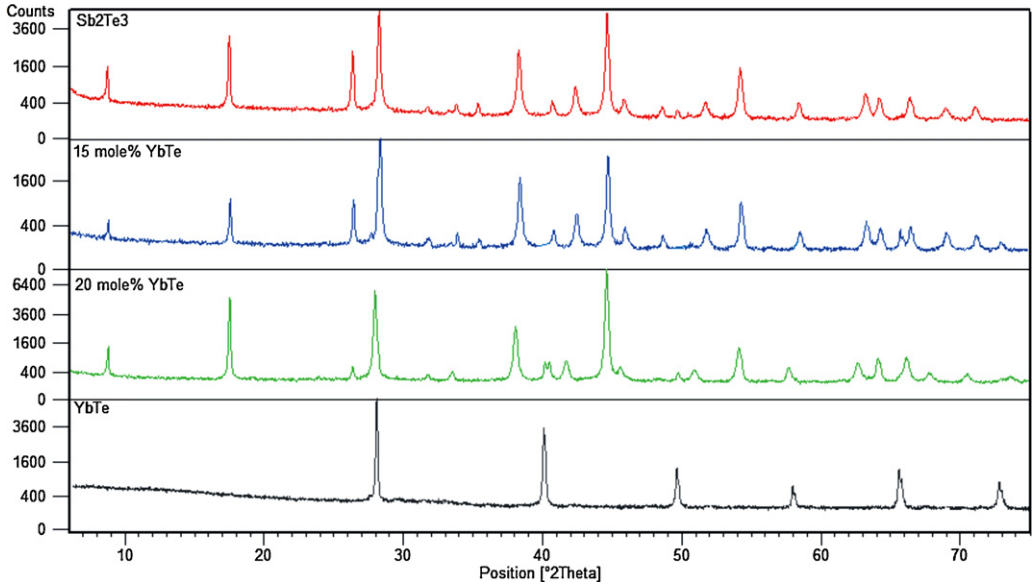

Fig. 2. XRD patterns for different compositions in the YbTe–Sb_2Te_3 system (color online).

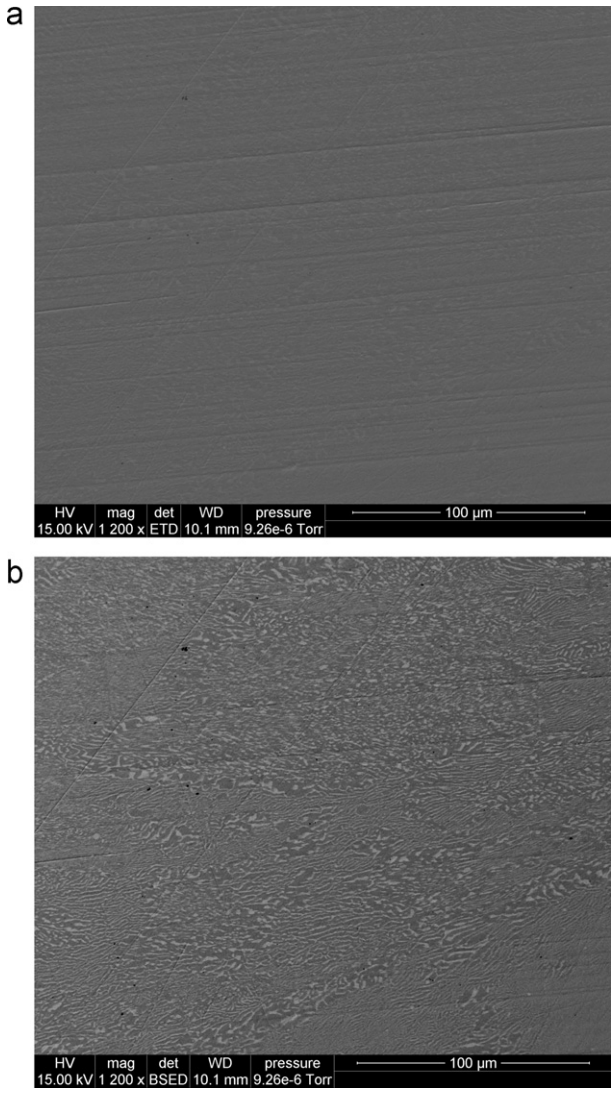

Fig. 3. SEM microphotographs of the alloys in the YbTe–Sb_2Te_3 system with 15 (a) and 20 (b) mol.% YbTe.

in the β-phase. It is clearly seen from Fig. 4 that the isotherms of the partial thermodynamic functions of YbTe have distinct kinks at 15 mol.% YbTe, the partial entropy exhibiting drastic changes near the limiting composition.

By integration of the Gibbs–Duhem equation

$$Z_{(YbTe)_x(Sb_2Te_3)_{1-x}} = (1-x)\int_0^x \frac{\overline{\Delta Z}_{YbTe}}{(1-x)^2}dx \quad (3)$$

($\Delta Z = \Delta G$ and ΔH; x is the molar fraction of YbTe in the alloys) the thermodynamic functions ΔG and ΔH of dissolution of YbTe in Sb_2Te_3 were calculated. The entropy of the dissolution was calculated using the Gibbs–Helmholtz equation:

$$\Delta S = \frac{\Delta H - \Delta G}{T} \quad (4)$$

The results of the calculations are shown in Table 3. By combining them with the corresponding thermodynamic data for YbTe and

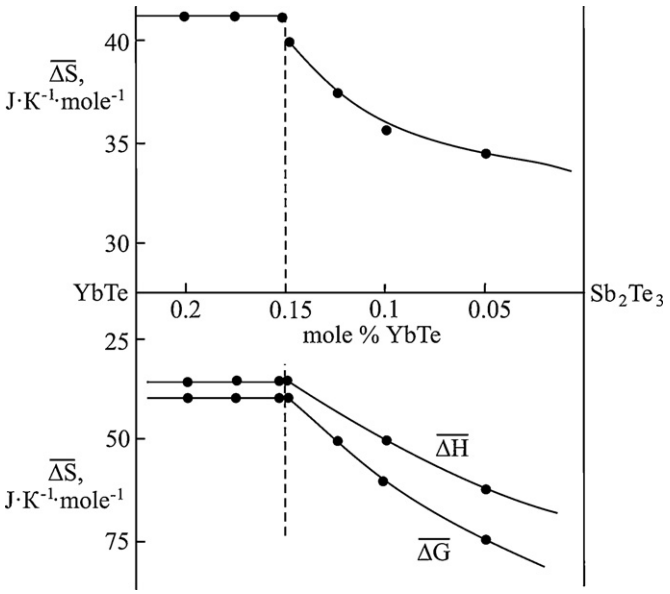

Fig. 4. Dependence of the relative partial thermodynamic functions of YbTe on the composition in the YbTe–Sb_2Te_3 system.

Table 3
Standard integral thermodynamic functions of the YbTe dissolution in Sb_2Te_3.

Composition	$-\Delta_s G^0$ (298) (kJ mol^{-1})	$-\Delta_s H^0$ (298) (kJ mol^{-1})	$\Delta_s S^0$ (298) (J K^{-1} mol^{-1})
$(YbTe)_{0.05}(Sb_2Te_3)_{0.95}$	4.37 ± 0.04	3.73 ± 0.16	2.15 ± 0.55
$(YbTe)_{0.1}(Sb_2Te_3)_{0.9}$	7.83 ± 0.06	6.61 ± 0.31	4.09 ± 0.92
$(YbTe)_{0.15}(Sb_2Te_3)_{0.85}$	10.03 ± 0.08	8.01 ± 0.46	6.78 ± 1.45

Table 4
Standard thermodynamic functions of formation and standard entropy of phases in the YbTe–Sb_2Te_3 system.

Compound	$-\Delta_f G^0$ (298) (kJ mol^{-1})	$-\Delta_f H^0$ (298) (kJ mol^{-1})	S^0 (298) (J K^{-1} mol^{-1})
Sb_2Te_3 [8,13]	56.9 ± 2.1	56.5 ± 1.3	246.4 ± 3.3
YbTe [12]	288.9 ± 0.5	297.8 ± 2.2	79.1 ± 7.1
$(YbTe)_{0.05}(Sb_2Te_3)_{0.95}$	72.9 ± 2.0	72.3 ± 1.4	239.8 ± 3.7
$(YbTe)_{0.1}(Sb_2Te_3)_{0.9}$	87.9 ± 1.9	87.2 ± 1.4	233.3 ± 4.1
$(YbTe)_{0.15}(Sb_2Te_3)_{0.85}$	101.7 ± 1.9	100.7 ± 1.5	227.2 ± 4.5

Sb_2Te_3 the standard integral thermodynamic functions of formation were calculated for the solid solution (β-phase). The estimated standard deviations were calculated by accumulating errors. It should be noted that the thermodynamic data for YbTe and Sb_2Te_3 used in this work are reliable (Table 4). The standard integral thermodynamic functions for YbTe were previously determined by the EMF method [8]. The standard enthalpy of formation and entropy for Sb_2Te_3 are similar to those given in modern reference books [14,15]. The standard Gibbs free energy calculated from these data agrees well with the results of the original study based on the EMF measurements [9].

3.3. Conclusions

The solubility of YbTe in Sb_2Te_3 is shown to have the limiting composition at 15 and 17.5 mol.% YbTe at 300 and 855 K, respectively, which is confirmed by a combination of the DTA, XRD, SEM, and EMF study. The solid solution (β-phase) retains the structural features of Sb_2Te_3. Partial relative thermodynamic functions of YbTe in the β-phase as well as the thermodynamic functions of dissolution of YbTe in Sb_2Te_3 were obtained based on the results of the EMF measurements. The calculated standard Gibbs free energy and enthalpy of formation of the β-phase are negative and show an increase of the absolute value with increasing the YbTe content, whereas the standard entropy shows an opposite trend.

References

[1] M.G. Kanatzidis, Acc. Chem. Res. 38 (2005) 361–370.
[2] A.V. Shevelkov, Russ. Chem. Rev. 77 (2008) 1–19, Uspekhi Khimii 77 (2008) 3–21.
[3] M.B. Babanly, J.-C. Tedenac, S.Z. Imamaliyeva, F.N. Guseynov, G.B. Dashdieva, J. Alloys Compd. 491 (2010) 230–236.
[4] T.F. Maksudova, O.A. Alieva, O.M. Aliev, Inorg. Mater. 24 (1988) 1191–1192.
[5] P.G. Rustamov, O.M. Aliev, T.F. Maksudova, Inorg. Mater. 17 (1981) 692–695.
[6] A.S. Guloy, F. Gascoin, A. Chamoire, J.-C. Tedenac, G.J. Snyder, Phys. Status Solidi (RRL) 1 (6) (2007) 265–267.
[7] L.E. Shelimova, O.G. Karpinskii, T.E. Svechnikova, E.S. Avilov, M.A. Kretova, V.S. Zemskov, Inorg. Mater. 40 (2004) 1264–1270.
[8] S.Z. Imamalieva, Z.S. Aliev, M.A. Mahmudova, M.B. Babanly, Az. Chem. Prob. 3 (2010) 453–456.
[9] M.B. Babanly, Yu.A. Yusibov, V.T. Abishov, EMF Method for Thermodynamics of the Composite Semiconductor Compounds, BSU, Baku, 1992, p. 327.
[10] M.B. Babanly, J.-C. Tedenac, Z.S. Aliyev, D.V. Balitsky, J. Alloys Compd. 481 (2009) 349–353.
[11] A.V. Shevelkov, E.V. Dikarev, R.V. Shpanchenko, B.A. Popovkin, J. Solid State Chem. 114 (1995) 379–395.
[12] K. Doerffel, Statistik in der analytischen Chemie, Grundstoffindustrie, Leipzig, 1990.
[13] A.N. Kornilov, L.B. Stepina, V.A. Sokolov, J. Phys. Chem. 46 (1972) 2975–2979.
[14] V.S. Yungman (Ed.), Data Base of Thermal Constants of Substances. Digital Version, 2006, http://www.chem.msu.su/cgi-bin/tkv.pl.
[15] O. Kubaschewski, C.B. Alcock, P.J. Spencer, Materials Thermochemistry, Pergamon Press, Oxford, 1993.